

NUMERICAL SIMULATION FOR HIGH- SPEED ALL- OPTICAL BOOLEAN GATES

Inmar N. Ghazi 

Abstract:

In this paper few high speed (i.e. as high as 80 GB/s) all-optical logic gates has been studied. These logic gates include a (80Gb/s XOR) gate using semiconductor optical amplifier (SOA) based Mach-Zehnder interferometer incorporated with a delayed interferometer (DI), The performance of XOR operation has been investigated using numerical simulations. The quality of the XOR result is improved using a (DI) delayed interferometer after the Mach-Zehnder interferometer. . A (80Gb/s XNOR) gate using four wave mixing (FWM) in highly nonlinear fibers (HNLF) have been studied also, the four wave mixing process is a very fast process in fibers ,the nonlinear Schrödinger equation that describes (FWM) process in fiber is solved numerically using the split-step Fourier transform method ,this scheme is capable of operating at a data rate as high as 250Gb/s ,finally A(40Gb/s) NOR gate operation has been analyzed by a numerical solution of the SOA rate equations. To investigate the quality of NOR operation by simulation, Q factor of the NOR output signal has been calculated. Q factor gives the information of the optical signal to noise ratio in digital transmission .All numerical simulation programs performed through Matt-Lab 7.0 prgram.

Key words:

All-Optical, logic gates, semiconductor optical amplifier (SOA), Mach-Zehnder interferometer, nonlinear Schrödinger equation, XOR gate, XNOR gate, NOR gate.

المحاكاة العددية للبوابات البصرية ذات السرعة العالية

الخلاصة:

في هذا البحث تم دراسة بعض البوابات المنطقية ذات السرعة العالية (أعلى من سرعة 80Gb/s) وتتضمن هذه البوابات بوابة (80Gb/s XOR) باستخدام المظخم البصري الشبه موصل (SOA) مستند على اساس منظومة التداخل نوع (Mach-Zehnder) مع منظومة التداخل التأخيرية (DI) حيث تم دراسة خواص البوابة (XOR) وذلك باستخدام المحاكاة العددية . ان اداء البوابة (XOR) قد تحسنت من خلال استخدام منظومة التداخل التأخيرية (DI) بعد منظومة التداخل (Mach-Zehnder) . وكذلك تم تحليل البوابة البصرية نوع (XNOR) ذات السرعة (80Gb/s) وذلك باستخدام المازج رباعي الموجة (FWM) في الليف البصري اللاخطي (HNLF) و استخدام معادلة شرويدر اللاخطية التي تصف عملية المازج الرباعي في الالياف ,وقد تم حلها عددياً باستخدام طريقة تحويل فوريير الخطوة المُقسمة (split-step Fourier transform method) . ان عملية المعالجة بالمازج الرباعي تمتاز بكونها معالجة سريعة جداً في الالياف البصرية وهذا المخطط قادر على التشغيل في نسبة بيانات بمعدل اعلى من (250Gb/s). واخيراً تم تحليل البوابة (40Gb/s NOR) وباستخدام مضخم بصري شبه موصل (SOA) وتحليل معادلات (SOA) النسبية عددياً . ولتحقيق الجودة لعمل بوابة (NOR) بالمحاكاة فقد تم حساب عامل الجودة (Q factor) للإشارة الخارجة من بوابة (NOR). ان عامل الجودة يعطي معلومات عن نسبة الضوضاء الى الإشارة (signal to noise ratio) في الارسال الرقمي .كل برامج المحاكاة العددية تم حلها بواسطة برنامج (مات لاب 7.0).

1. INTRODUCTION:

The optical communication system does not work entirely in optical domain. A large amount of the switches and data processors are made of electrical circuits. The bandwidth of the electrical circuits limits the ultimate speed of the existing light wave transmission systems. A promising solution is to migrate from the electrical parts to optical parts. A key building block of data processing and switching is the all optical Boolean functions such as NOR, XNOR, XOR, and circuits made using these building blocks. It is important to build all-optical logic gates with the following qualities: (1) high-data rate operation (2) low noise (3) WDM (wavelength-division multiplexing) capability. Previous attempts have been made to realize all-optical Boolean functions [1, 2, 3, 4, and 5] by using semiconductor optical amplifier (SOA) and fiber based devices. The bandwidth of the demonstrated logic gates built on SOA is limited by SOA carrier lifetime. In order to further enhance operation speed, fast semiconductor optical devices are desired. This became possible when quantum dot SOAs (QD-SOA) and carrier reservoirs SOAs (CR-SOA) are invented in late 1990s [3]. Because of their unique band structure and density of states, these kinds of SOAs are more than 10 times faster in signal response time. This suggests that such devices may be capable of handling data at bit-rate up to 250 Gb/s. The all optical Boolean functions can be implemented in various data processing systems such as binary adder [1, 2], decision circuits [5], bit pattern generation [6], optical head processing [7,8], and packet switching

[2]. the tradeoff of the all optical data processing solutions are having larger noise and more power consumption than electrical counterparts.

In this work, theoretical demonstration of XOR, XNOR and OR gates will be carried out. The operating speed of the logic gates reaches as high as 80 Gb/s up to 250 Gb/s, these ultra high speed logic operations employed the various techniques such as SOA-MZI-DI, four wave mixing (FWM) in highly nonlinear optical fiber (FINLF). processing solutions are having low noise & higher speed. The details of setup principles and results are discussed in details accordingly.

2. 80 Gb/s XOR using SOA-MZI-DI

In the case of XOR operation, SOA based MZI is generally used because it is compact and stable. However, conventional techniques using SOA-MZI are limited by the gain and phase response time of SOA (i.e., 50-200ps), which limits the operating speed to 20Gb/s. Various differential schemes have been proposed and realized [6,2,9] to overcome the speed limitation. A scheme which utilizes a DI (delayed interferometer) after SOA-MZI has been proposed in [2]. In this work, XOR function is achieved theoretically verification of the scheme has been carried out using a rate equation model.

2.1. NUMERICAL SIMULATION:

XOR gate operation has been analyzed by a numerical solution of the SOA rate equations. The time dependent gain of the SOA satisfies the temporal gain rate equations [8, 2] from (1) to (3).

$$\frac{dh_1(t)}{dt} = \frac{h_0 - h_1(t)}{\tau_c} - \frac{S(t,0)}{E_{sat}} [e^{h_{total}} - 1] \dots (1)$$

$$\frac{dh_{CH}}{dt} = -\frac{h_{CH}}{\tau_{CH}} - \frac{\varepsilon_{CH}}{\tau_{CH}} [e^{h_{total}} - 1] S(t,0) \dots (2)$$

$$\frac{dh_{SHB}}{dt} = -\frac{h_{SHB}}{\tau_{SHB}} - \frac{\varepsilon_{SHB}}{\tau_{SHB}} [e^{h_{total}} - 1] \times S(t,0) - \frac{dh_l}{dt} - \frac{dh_{CH}}{dt} \dots (3)$$

In above equations, $h_l(t)$ is a integral of optical gain over the length of SOA and h_{total} equals the sum of h_l , h_{CH} and h_{SHB} , where h_l , h_{CH} , h_{SHB} are the h-factor values for carrier recombination, carrier heating and spectral hole burning respectively. τ_C is the carrier lifetime, τ_{CH} is the carrier heating lifetime and the τ_{SHB} is the spectral hole burning lifetime, h_0 is the h-factor of the unsaturated power gain where the $\text{Exp}[h_0] = G_0$ and E_{sat} is the saturation energy of the SOA. $S(t,0)$ is the instantaneous input optical intensity inside the SOA and ε_{CH} is the gain suppression factor owing to carrier heating effect, ε_{SHB} is the gain suppression factor owing to spectral hole burning effect. Equations (1), (2) accounts for the intra-band carrier dynamics (i.e. spectral hole burning and carrier heating effects). Here, we assume the data stream pulses to be Gaussian pulses, [9]. So,

$$P_{A,B}(t) = \sum_{n=-\infty}^{+\infty} a_{nA,B} \frac{2\sqrt{\ln 2 P_0}}{\sqrt{\pi\tau_{FWHM}}} \times \exp\left(-\frac{4 \ln 2 (t - nT)^2}{\tau_{FWHM}^2}\right) \dots (4)$$

where P_0 is the energy of a single pulse, $a_{nA,B}$ represents nth data in data stream A and B, $a_{nA,B} = 1$ or 0 , τ_{FWHM} is full width of half maximum pulse width.

To simulate the XOR gate performance, we assume both input signals are of RZ (return-to-zero) format pseudorandom bit sequence. The carrier density induced phase change is described by [10]:

$$\phi(t) = -\frac{1}{2} [\alpha_d(t) + \alpha_{CH} h_{CH}(t)] \dots (5)$$

where α is the linear line width enhancement factor (i.e. $\alpha = 4$), α_{ch} is the carrier heating alpha factor (i.e. $\alpha_{ch} = 1$), other SOA parameters are as follows: $G_0 = 30\text{dB}$, $\tau_c = 20\text{ps}$, $\tau_{FWHM} = 2\text{ps}$, $\tau_{SHB} = 100\text{fs}$, $\tau_{CH} = 300\text{fs}$, $\varepsilon_{SHB} = \varepsilon_{CH} = 0.08\text{ps}$.

3. 80Gb/s XNOR using FWM in HNLF

In the case of XNOR operation, four wave mixing (FWM) in high nonlinear fiber (HNLF) is used. The four wave mixing process is a very fast process in fibers. For pulses longer than 100fs it is nearly instantaneous [11]. Validity of this assumption guarantees a high data rate operation in a fiber FWM based system. Theoretical calculation is also presented using the split-step Fourier transform method, the nonlinear Schrödinger equation that describes FWM process in fiber is solved numerically. Estimated speed of the transmission rate for our scheme is $\approx 250 \text{ GB/s}$.

3.1 NUMERICAL SIMULATION:

A numerical model of the XNOR process based on FWM is described in this paper. The nonlinear Schrödinger equation (NLS) is used to describe nonlinear process in the fiber. The following equations [3] are the coupled NLS for FWM in HNLF, assuming that the phase matching condition is perfectly satisfied along all the fiber length.

$$\frac{\partial A_1}{\partial z} + \beta_{11} \frac{\partial A_1}{\partial t} + \frac{i}{2} \beta_{21} \frac{\partial^2 A_1}{\partial t^2} = i\gamma \times \left[(|A_1|^2 + 2|A_2|^2 + 2|A_3|^2 + 2|A_4|^2) A_1 + 2A_2^* A_3 A_4 e^{-i\gamma(P_1 + P_2)z} \right] \dots (6)$$

$$\frac{\partial A_2}{\partial z} + \beta_{12} \frac{\partial A_2}{\partial t} + \frac{i}{2} \beta_{22} \frac{\partial^2 A_2}{\partial t^2} = i\gamma \times \left[(|A_2|^2 + 2|A_1|^2 + 2|A_3|^2 + 2|A_4|^2) A_2 + 2A_1^* A_3 A_4 e^{-i\gamma(P_1 + P_2)z} \right] \dots (7)$$

$$\frac{\partial A_3}{\partial z} + \beta_{13} \frac{\partial A_3}{\partial t} + \frac{i}{2} \beta_{23} \frac{\partial^2 A_3}{\partial t^2} = i\gamma \times \left[(|A_3|^2 + 2|A_1|^2 + 2|A_2|^2 + 2|A_4|^2) A_3 + 2A_4^* A_1 A_2 e^{i\gamma(P_1 + P_2)z} \right] \dots (8)$$

$$\frac{\partial A_4}{\partial z} + \beta_{14} \frac{\partial A_4}{\partial t} + \frac{i}{2} \beta_{24} \frac{\partial^2 A_4}{\partial t^2} = i\gamma \times \left[(|A_4|^2 + 2|A_1|^2 + 2|A_2|^2 + 2|A_3|^2) A_4 + 2A_3^* A_1 A_2 e^{i\gamma(P_1 + P_2)z} \right] \dots (9)$$

In above equations β_1 is the inverse of group velocity and β_2 is linearly proportional to chromatic dispersion parameter of the fiber. γ is the nonlinear coefficient of the fiber medium. P_1 and P_2 are input signal powers (i.e. $|A_1(0)|^2$ and $|A_2(0)|^2$), and $A_i(z, t)$ is the pulse amplitude for input signal and FWM generated pulses. In our case, β_2 is as follows: $\beta_{21} = 0$, $\beta_{22} = 0.06$, $\beta_{23} = -0.06$, and $\beta_{24} = 0.09$. Because the zero dispersion point is around 1555nm in our HNLF the dispersion slope is flat at around 0.019ps/nm/nm/km. γ , the nonlinear coefficient of our HNLF, is $10.5(\text{W}^{-2}\text{km}^{-2})$.

4

Considering the propagation in a retarded frame in which $T = t - z/v_g$, v_g is group velocity, the first order time derivative term can be neglected in our calculation. Assuming that input pulse trains are non-chirp Gaussian type pulses, its amplitude can be expressed as follows:[3]

$$A_i(0, t) = \sqrt{P_i} \sum_n a_n \exp \left[-\frac{(t - nT)^2}{t_{FWHM}^2} \right] \dots (10)$$

$a_n = 1$ or 0, T is the pulse train period

(i.e. 80Gb/s $T=12.5\text{ps}$, 160Gb/s $T=6.25\text{ps}$), and t_{FWHM} is the full width half maximum of pulse train which is 2ps in our simulation. P is the peak power of input signal; we take it as 2W for 80Gb/s pulse. The above set of NLSs can be numerically solved by split-step Fourier method [3]

4. 40Gb/s NOR using SOA-MZI:

All-optical NOR gates can be formed by cascading an all-optical OR gate and an INVERT operation at ≈ 80 Gb/s have been demonstrated previously using a semiconductor optical amplifier (SOA) followed by a delayed interferometer (DI) [12, 13]. The performance of the NOR results are numerically analyzed by solving the gain and phase rate equation of an SOA

4.1 NUMERICAL SIMULATION:

The NOR gate operation has been analyzed by a numerical solution of the SOA rate equations. As shown in Figure (1), the pump signals A and B are combined and launched into the upper SOA, while the 40 GHz optical clock is injected into the lower SOA; thus the sum of signal A and B will modulate the gain of upper SOA together and thereby the phase of the probe signal(CW). Similarly, in the lower arm, the phase of the probe signal is modulated by the injection of clock signal. At the output stage of the MZI,

the probe signal out of both SOAs interferes and the NOR output intensity is given by:[10]

$$P_{\text{NOR}} = \frac{P_{\text{CW}}}{4} \left\{ \frac{G_1(t) + G_2(t) - 2\sqrt{G_1(t)G_2(t)} \times \cos[\phi_1(t) - \phi_2(t)]}{2} \right\} \dots\dots\dots (11)$$

where P_{CW} represents the CW power before SOAs, $G_{1,2}$ is the time-dependent gain of SOA and $\phi_{1,2}$ is the phase shift in the SOA.

Note that the origin of phase shift is rooted in the gain modulation of SOA, therefore, assuming the phase shift $\phi(t)$ is linearly related to the gain $G(t)$ in SOA by the line width enhancement factor.

Let us define $h(t)$ as follows,[4]

$$G(t, z) = \text{Exp}(h(t)) \dots\dots\dots (12)$$

Where,

$$h(t) = \int_0^L g(t, z) dz \dots\dots\dots (13)$$

By taking into consideration carrier heating and spectral hole burning effects, the time- dependent gain for each SOA is given by the following equations [6,7,8].

$$\frac{dh_N}{dt} = \frac{h_0 - h_N}{\tau_c} - [\text{Exp}(h_N + h_{\text{CH}} + h_{\text{SHB}}) - 1] S(t, 0) \dots\dots\dots (14)$$

$$\frac{dh_{\text{CH}}}{dt} = -\frac{h_{\text{CH}}}{\tau_{\text{CH}}} - \frac{\varepsilon_{\text{CH}}}{\tau_{\text{CH}}} \left[\text{Exp} \left(\frac{h_N + h_{\text{CH}}}{h_{\text{SHB}}} \right) - 1 \right] S(t, 0) \dots\dots\dots (15)$$

$$\frac{dh_{\text{SHB}}}{dt} = -\frac{h_{\text{SHB}}}{\tau_{\text{SHB}}} - \frac{\varepsilon_{\text{SHB}}}{\tau_{\text{SHB}}} [\text{Exp}(h_N + h_{\text{CH}} + h_{\text{SHB}}) - 1] \times S(t, 0) - \frac{dh_N}{dt} - \frac{dh_{\text{CH}}}{dt} \dots\dots\dots (16)$$

In the above equations,

$$h_0 = \Gamma g_i (N_{\text{st}}) L = \Gamma a (N_{\text{st}} - N_{\text{tr}}) L \dots\dots\dots (17)$$

$$G(t, z) = \text{Exp}[h_N + h_{\text{SHB}} + h_{\text{CH}}] \dots\dots\dots (18)$$

where h_N , h_{CH} , h_{SHB} are the h -factor values for carrier recombination, carrier heating and spectral hole burning, respectively; τ_c is the carrier lifetime,

τ_{CH}^{-1} is the temperature relaxation rate,

τ_{SHB}^{-1} is the carrier-carrier scattering

rate, ε_{SHB} and ε_{CH} are the nonlinear gain suppression factors due to carrier heating and spectral hole burning, and g_0 is the unsaturated power gain. $S_{1,2}$ is the instantaneous optical intensity inside each SOA respectively, namely,

$$S_1(t) = S_A(t) + S_B(t) + S_{\text{CW}} \dots\dots\dots (19)$$

$$S_2(t) = S_{\text{CLK}}(t) + S_{\text{CW}} \dots\dots\dots (20)$$

$$P_{1,2}(t) = k S_{1,2}(t) \dots\dots\dots (21)$$

where k denotes the conversion factor from photon density to power, therefore,

$$P_1(t) = P_A(t) + P_B(t) + P_{\text{CW}} \dots\dots\dots (22)$$

$$P_2(t) = P_{\text{CLK}}(t) + P_{\text{CW}} \dots\dots\dots (23)$$

The line width enhancement factor (α -factor) for different processes (e.g. band-to-band transition,

carrier heating and spectral hole burning) are different [14]. The carrier density induced phase change is described by:[10]

$$\phi(t) = -\frac{1}{2}[\alpha h_d(t) + \alpha_{CH} h_{CH}(t)] \dots \dots \dots (24)$$

where α is the regular line width enhancement factor (i.e. $\alpha \approx 4$), α_{CH} is the carrier heating alpha factor (i.e. $\alpha_{CH}=1$). The a-factor for spectral hole burning is 0.

We assume the data stream pulse to be Gaussian pulses with FWHM pulse width of 1/8 bit period, e.g. $\tau_{FWHM} = T/8$.

i.e. [9] ;

$$P_{A,B}(t) = \sum_{n=-\infty}^{+\infty} a_{nA,B} \frac{2\sqrt{\ln 2P_0}}{\sqrt{\pi}\tau_{FWHM}} \times \exp\left(-\frac{4\ln 2(t-nT)^2}{\tau_{FWHM}^2}\right) \dots \dots \dots (25)$$

where P_0 is the single pulse energy, and A,B represents nth data in data stream A and B, an A,B= 1 or 0. In this simulation work, we assume both SOAs in the MZI have the same operating conditions. The parameters of SOAs are as follows,

$\tau_C = 40\text{Ps}$, $\tau_{SHB} = 100\text{fs}$, $\tau_{CH} = 300\text{fs}$, $\epsilon_{SHB} = \epsilon_{CH} = 0.08$, line width enhancement factor $\alpha = 4$, amplifier maximum gain = 20dB, injected current density = $4\text{kA}/\text{cm}^2$.

5. RESULTS & DISCUSSION

5.1 80Gb/s XOR using SOA-MZI-DI

Figure (2) shows the calculated XOR results using the above equations, signal A has (01100110) pattern, and signal B has (11001100) pattern. Signals A and B are on the left figure and the XOR output is on the right. Figure (3a) illustrates the XOR operation without PML-DI using the above equations. Signals A and B are of $2^7 - 1$ pseudorandom bit patterns. In the simulation, the input powers of the two signals are equal, and, the saturated gain values for the two wavelengths are also equal. Figure (3b) shows the simulated result of XOR operation with PML-DI. An undesired side-pulse emerges in this scheme.

This phenomenon is a result of carrier recovery processes in SOA [2]. At the receiving end of XOR, the side pulse can be filtered out using a low pass filter. The calculated Q value after filter is larger with DI than without DI. We believe the operating speed limit is $\approx 100 \text{ Gb/s}$ for the bulk active SOA gain and phase response parameters used here. For MZI utilizing fast SOA i.e. SOA with fast gain and phase recovery times, (such as quantum dot SOA), the operating speed is $\approx 250 \text{ Gb/s}$ [10].

The simulated XOR output using MZI followed by DI and MZI alone are shown in Figures (2) and (3). The simulation also shows a performance improvement (higher Q) if the MZI is followed by a DI. The simulation results for pseudorandom pulses suggest $Q > 6$ with DI.

5.2 80Gb/s XNOR using FWM in HNLF

Figure (4) shows the calculated result of 80Gb/s $2^7 - 1$ pseudorandom XNOR result, quality factor Q is calculated as 12.8. We also carried out the simulation for 250Gb/s for $2^7 - 1$ pseudorandom pulse pattern. Figure (5) is the calculated eye diagrams for XNOR, output at 80Gb/s and 250Gb/s. The Q value drops to 6.9 at 250Gb/s, we believe that this is due to pulse-broadening effect which leads to bit overlap. For a shorter pulse width, higher speed of XNOR operation is expected.

5-3 40 Gb/s NOR using SOA-MZI

Figure (6) shows the simulation results of NOR gate operation, (i) and (ii) shows (11001100) pattern of signal A and (01100110) pattern of signal B, respectively. The incoming 40Gb/s clock is shown in Figure (6) (iii), and the bottom trace (Figure (6) (iv)) shows the NOR output after MZI. To investigate the "quality" of NOR operation by simulation, Q factor of the NOR output signal has been calculated. Q factor gives the information of the optical signal to noise ratio in digital transmission. We analyze the Q factor following Ref. [15]. Q is defined by,

$$Q = \frac{P_1 - P_0}{\sigma_1 + \sigma_0} \dots\dots\dots (26)$$

where P_1 and P_0 are the average power of "1" and "0" signal respectively in the output NOR data stream, while σ_1 and σ_0 are the standard deviation of 1's and

0's. The input patterns in this case are $2^7 - 1$ pseudorandom data pattern.

6- CONCLUSION

In this paper, an all-optical XOR gate at 80 Gb/s has been demonstrated based on a semiconductor optical amplifier – Mach-Zehnder-interferometer and delayed interferometer (DI) device. We investigated the performance of XOR operation using numerical simulations. The quality of the XOR result is improved using a DI after the Mach-Zehnder interferometer.

A novel differential FWM XNOR scheme based on HNLF has been proposed and demonstrated.

A nonlinear Schrödinger equation model is utilized to simulate the FWM process. Based on numerical calculation, this scheme is capable of operating at a data rate as high as 250 Gb/s.

40 Gb/s NOR gate based on the SOA-MZI device has been demonstrated. By solving the rate equation of SOA, we investigated the NOR performance numerically. Q - factor increases if the input signals are larger.

References:

1. J. Leuthold, C. Joyner, B. Mikkelsen, G. Raybon, J. Pleumeekers, B. Miller, K. Dreyer, and C. Burrus, "100 Gbit/s all-optical wavelength conversion with integrated SOA delayed-interference configuration", *Electron. Lett.*, vol. 36, pp.1129-1130, 2000.
2. S.Randel,A.Marques de Melo, K.Petermann, V.Marembert and C.Schubert "Novel Scheme for Ultrafast All-Optical XOR operation", *IEEE Journal of Lightwave Technol.* Vol.22, pp. 2808-2815, 2004.
3. G.P. Agrawal," Nonlinear Fiber Optics", 3rd edition, Academic Press, 2001
4. M. Zhang, Y. Zhao, L. Wang, J. Wang and P. Ye, "Design and analysis of all-optical gate using SOA-based Mach-Zehnder interferometer", *Optics Communications* 223 301-308, 2003
5. A. Sharaiha, H. W. Li, F. Marchese , J. LeBihan , "All-optical logic NOR gate using a semiconductor laser amplifier", *Electronics Letters*, 33 (4): 323-325 Feb 1997.
6. T.Houbavlis, K.Zoiros, K.Vlachos, T.Papakyriakopoulos, H.Avrampoulos, F. Girardin, G. Guekos, R. Dall'Ara, S. Hansmann, andH. Burkhard, "All-optical XOR in a semiconductor optical lifierassisted fiber Sagnac gate," *IEEE Photon. Technol. Lett.*, vol. 11, pp.334-336, Mar. 1999.
7. C. Bintjas, M.Kalyvas,G.Theophilopoulos, T. Stathopoulos, H.Avrampoulos, L. Occhi, L. Schares, G. Guekos, S. Hansmann, andR. Dall'Ara, "20 Gb/s all-optical XOR with UNI gate," *IEEE Photon.Technol. Lett.*, vol. 12, pp. 834-836, July 2000
8. R. P.Webb, R. J. Manning, G. D. Maxwell, and A. J. Poustie, "40 Gbit/sall-optical XOR gate based on hybrid-integrated. Mach-Zehnder interferometer,"*Electron Lett.*, vol. 39, no. 1, pp. 79-81, 2003.
9. Q. Wang, G. Zhu, H. Chen, J. Jaques, J. Leuthold, A. B. Piccirilli, and N. K. Dutta, "Study of all-optical XOR using Mach-Zehnder interferometer and differential scheme," *IEEE J.Quantum Electron.*, Vol.40, pp.703-710,2004.
10. H. Sun, Q. Wang, H. Dong and N. K. Dutta "XOR Performance of a Quantum Dot Semiconductor Optical Amplifier Based Mach-Zehnder Interferometer" *Optics Express*, Vol.13, 1892-1899, March 2005
11. D.L.Hart, A.F. Judy, R. Roy and J.W. Beletic, "Dynamical evolution of multiple four-wave-mixing process in an optical fiber", *Physical Review E*, Vol. 57, No.4 pp4757-4774, Apr.1998
12. H. Dong, Q. Wang, G. Zhu, J. Jaques, A.B. Piccirilli and N.K. Dutta, "Demonstration of all-optical logic OR gate using semiconductor optical amplifier-delayed interferometer," *Opt. Commun.* vol.242, pp479-485, Dec. 2004.
13. C. Zhao, X. Zhang, H. Liu, D. Liu, and D. Huang, "Tunable all-optical NOR gate at 10Gb/s based on SOA fiber ring laser," *Opt. Express*, vol.13, no. 8, pp. 2783-2798, 2005.
14. G.P. Agrawal, N.K. Dutta, "Semiconductor Lasers", Kluwer Academic Publishers; 2nd edition June 1993
15. R. Gutierrez-Castrejon, L. Occhi, L. Schares, and G. Guekos, "Recovery dynamics of cross-modulated beam phase in semiconductor amplifiers and applications to all-optical signal processing", *Optics Communications*, 195 (1), p.167-177, Aug 2001.

Appendix A

A.1. Nonlinear Schrödinger Equation

$$\frac{\partial A_i^x}{\partial z} + \frac{1}{v_{gi}} \frac{\partial A_i^x}{\partial t} + \frac{j}{2} \beta_{2i} \frac{\partial^2 A_i^x}{\partial t^2} - \frac{1}{6} \beta_{3i} \frac{\partial^3 A_i^x}{\partial t^3} + \frac{\alpha_i}{2} A_i^x = \hat{N}(A_i^x \dots; A_i^y \dots) \dots \dots \dots (A.1)$$

$$\frac{\partial A_i^y}{\partial z} + \frac{1}{v_{gi}} \frac{\partial A_i^y}{\partial t} + \frac{j}{2} \beta_{2i} \frac{\partial^2 A_i^y}{\partial t^2} - \frac{1}{6} \beta_{3i} \frac{\partial^3 A_i^y}{\partial t^3} + \frac{\alpha_i}{2} A_i^y = \hat{N}(A_i^x \dots; A_i^y \dots) \dots \dots \dots (A.2)$$

A_i^x and A_i^y are the complex modal amplitudes of the i th channel. For single-channel mode simulations, only a single amplitude is used for each polarization. Further, v_{gi} is the group velocity β_{2i} is the second-order dispersion coefficient, β_{3i} is the third-order dispersion coefficient, evaluated at the center wavelength and α_i is the frequency dependent attenuation coefficient. The nonlinear response is represented by the terms \hat{N}_x and \hat{N}_y [1].

A.2. Split step Fourier treatment

The nonlinear Schrödinger Equation (NLSE) is usually solved using a split step Fourier transform method. The idea is to separate the linear dispersive operator \hat{D} and nonlinear operator \hat{N} in the equation. The NLSE A.1 and A.2 can be seen as:

$$\frac{\partial A}{\partial z} = (\hat{D} + \hat{N})A \dots \dots \dots (A.3)$$

It is assumed that the nonlinear operator and the linear dispersive operator affect the optical wave amplitude intermittently. The interval is the step size used during calculation, the smaller the more accurate. Following is an example flow chart Figure A.1 of the calculation

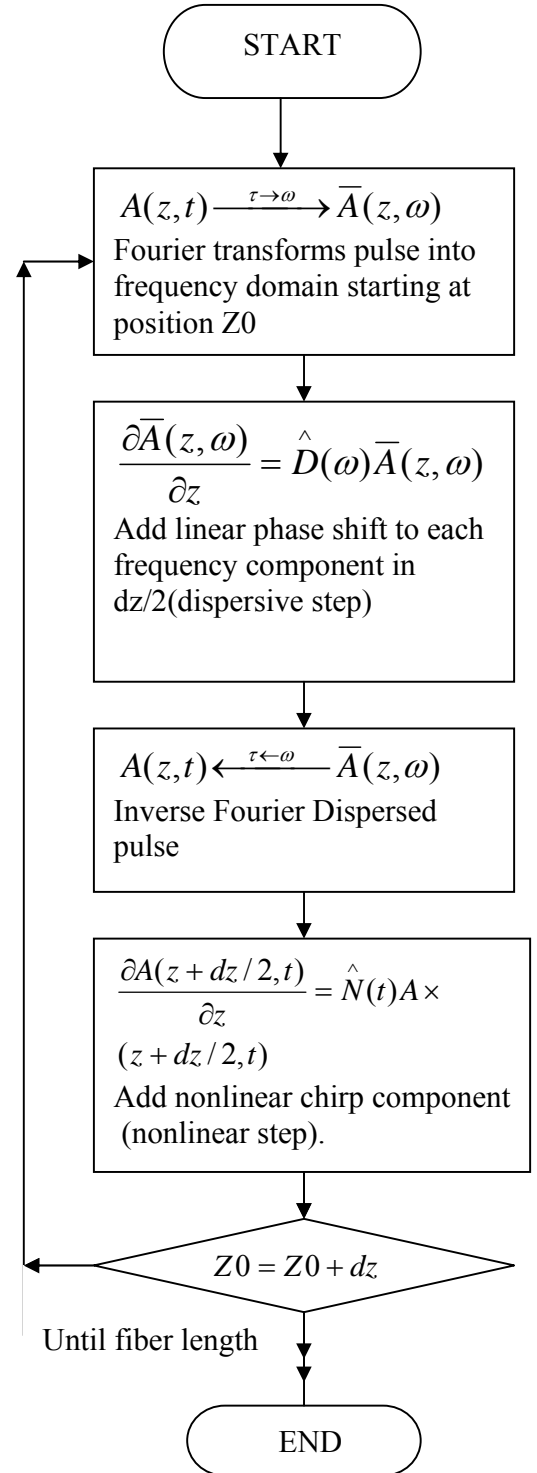


Fig A.1 Flow chart of split step Fourier method used in solving NLSE, is performed through MatLab 7.0 program.

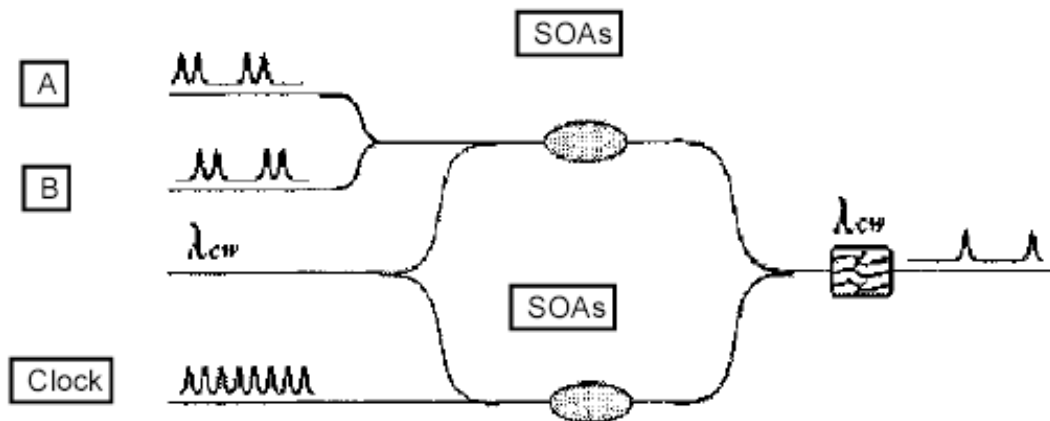


Figure (1): schematic diagram of the SOA-MZI as the NOR gate. signals A&B (combined)are injected into one SOA& clock signal is injected into the second SOA.

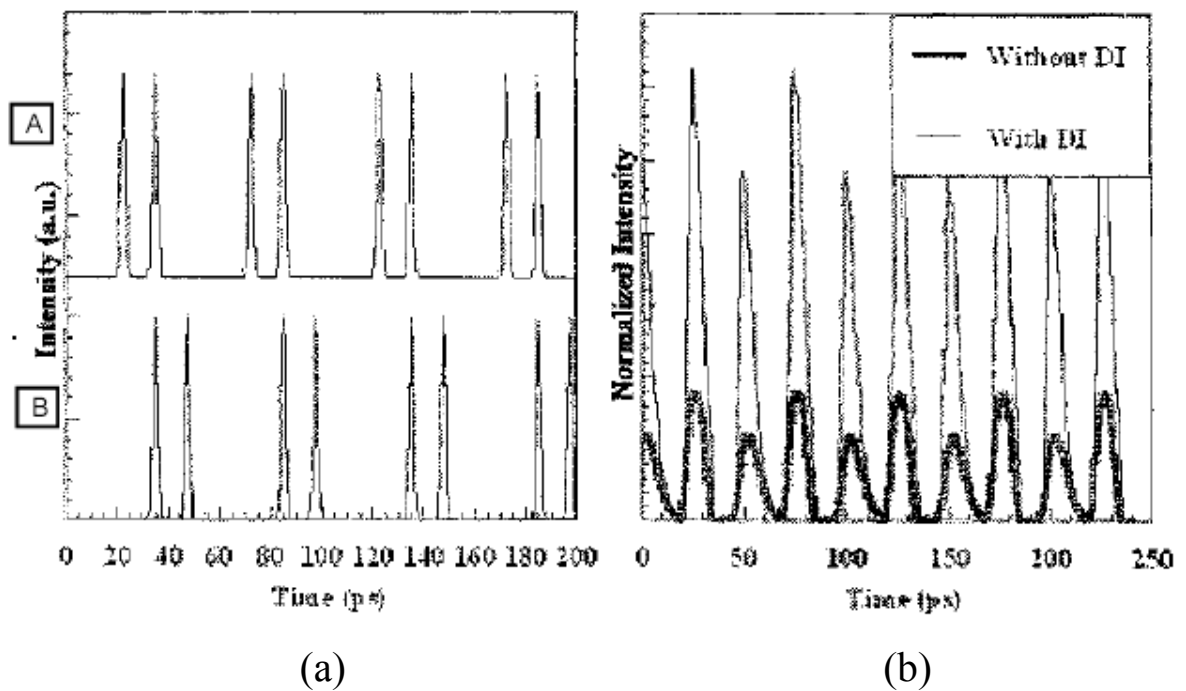


Figure 2: (a) Input 80Gb/s patterns (b) Comparison of XOR output before and after PML-DI. . Signals A and B are on the left figure and the XOR output is on the right.

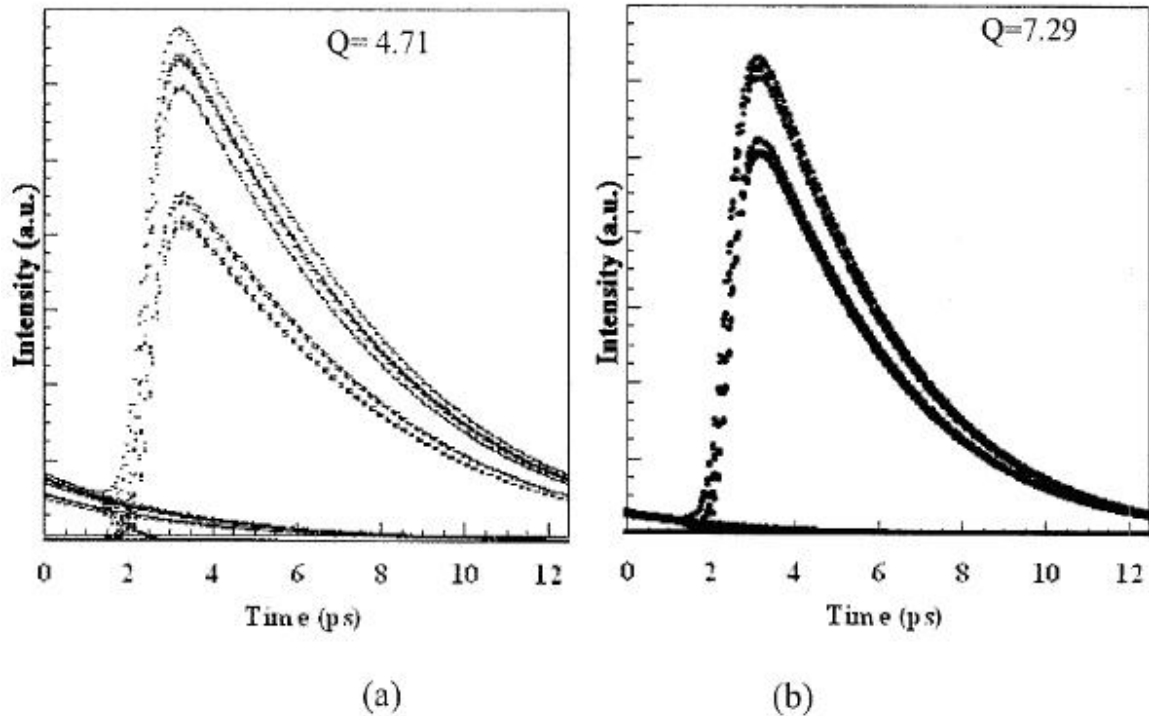


Figure 3: (a) Simulated XOR eye-diagram with MZI alone (without DI) with input 80Gb/s pseudorandom pattern (b) eye-diagram with MZI followed by DI after low pass filter (The inset shows side pulse before filter and is in the same scale as in large figure)

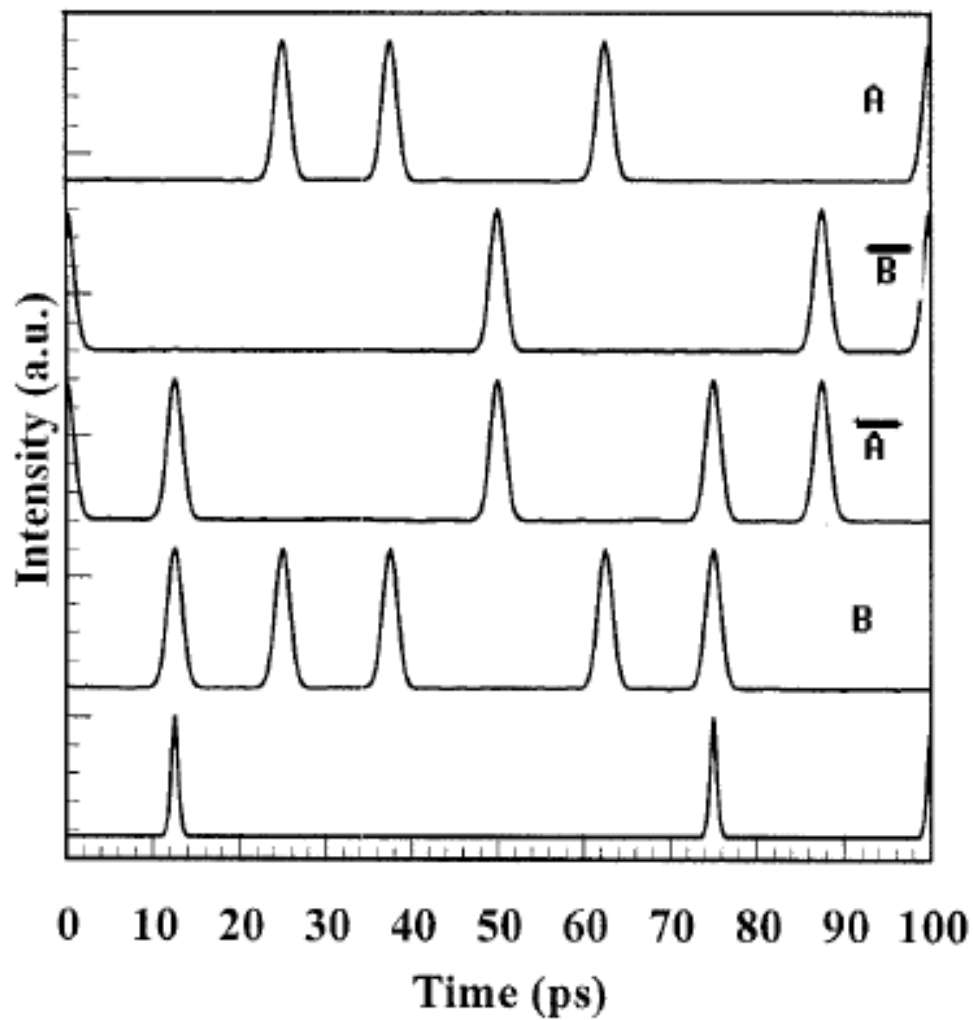


Figure 4; Simulated XNOR result at 80Gb/s

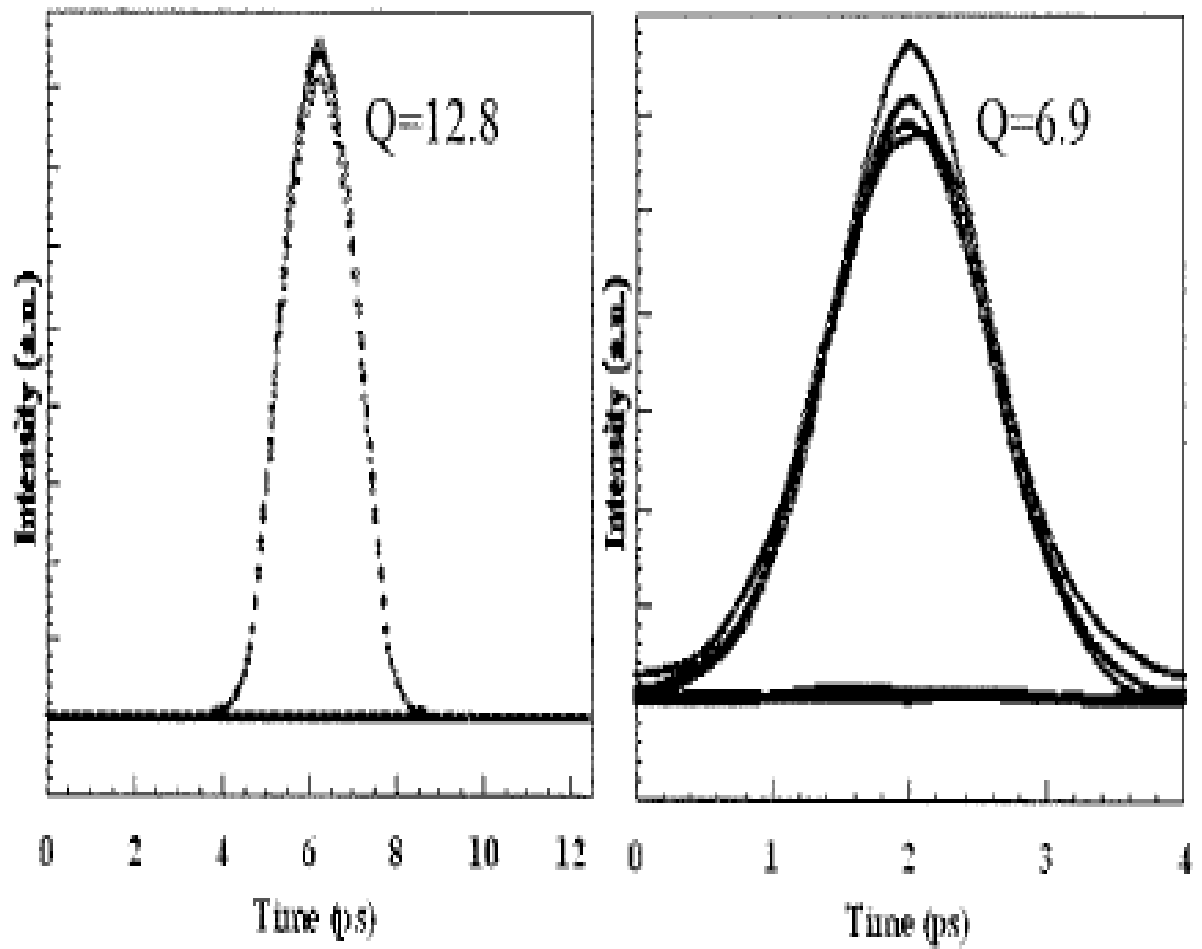


Figure 5: Eye diagram for 2^7-1 pseudorandom bit pattern input at 80Gb/s (left) and 250 Gb/s (right)

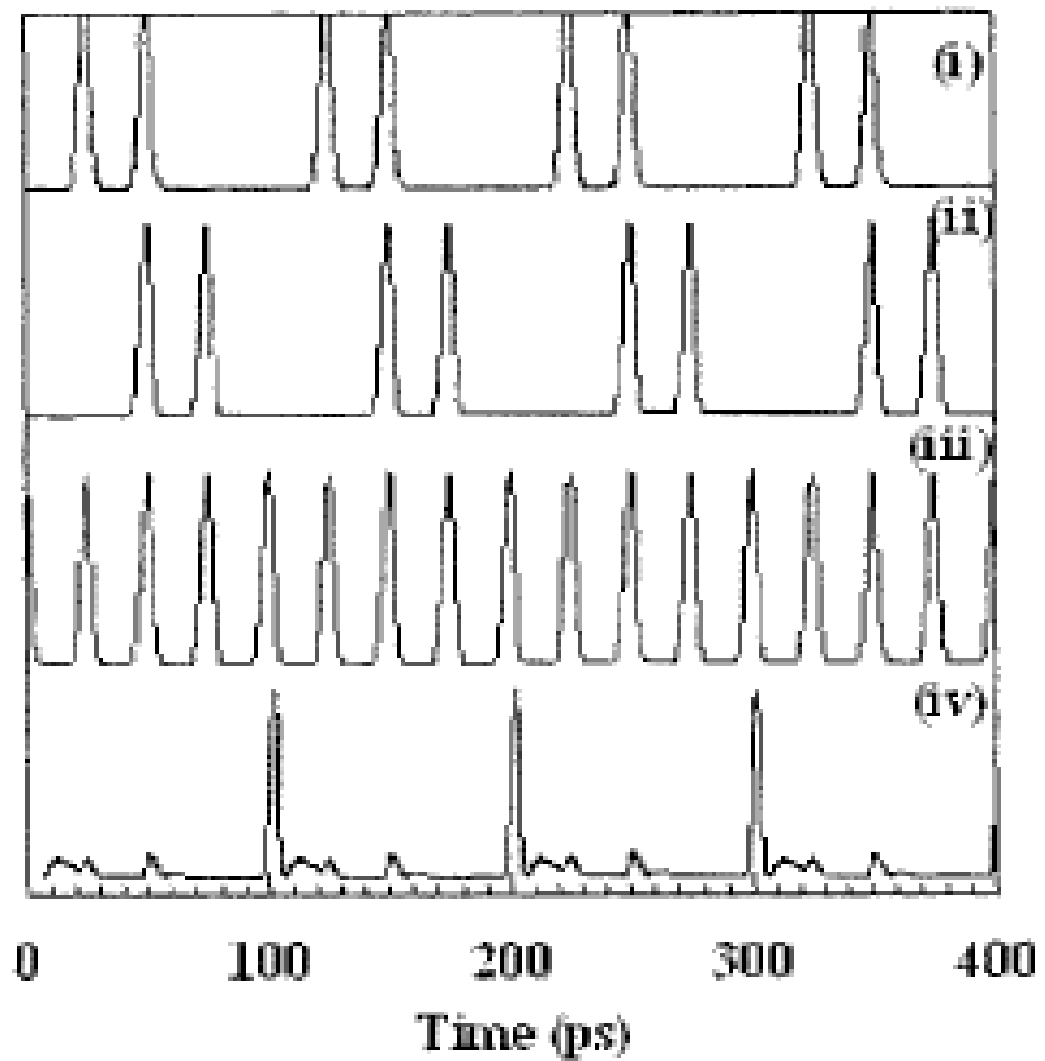


Figure 6: The simulated results of SOA-MZI output as a response to the patterned 40Gb/s input of 11001100 and 01100110. (i) – Signal A, (ii)) Signal B , (iii) Clock , (iv) NOR output from MZI

